IOPscience iopscience.iop.org

Home Search Collections Journals About Contact us My IOPscience

Laser-Ablation-Induced Concentric Ring Structures

This content has been downloaded from IOPscience. Please scroll down to see the full text.

2003 Jpn. J. Appl. Phys. 42 5123

(http://iopscience.iop.org/1347-4065/42/8R/5123)

View the table of contents for this issue, or go to the journal homepage for more

Download details:

IP Address: 128.192.114.19
This content was downloaded on 06/09/2015 at 19:44

Please note that terms and conditions apply.

Jpn. J. Appl. Phys. Vol. 42 (2003) pp. 5123–5126
Part 1, No. 8, August 2003
©2003 The Japan Society of Applied Physics

Laser-Ablation-Induced Concentric Ring Structures

Bin LAN, Ming-Hui HONG*, Shi-Xin CHEN[1], Kai-Dong YE, Zeng-Bo WANG[1], Guo-Xin CHEN[1] and Tow-Chong CHONG

Data Storage Institute, DSI Building, 5 Engineering Drive 1, (off Kent Ridge Crescent, NUS), 117608, Singapore
[1]*Electrical and Computer Engineering Department, National University of Singapore, 10 Kent Ridge Crescent, 119260, Singapore*

(Received September 25, 2002; accepted for publication March 26, 2003)

Formation of concentric ring structures on substrate surface by 3rd harmonic Nd:YAG laser ablation is investigated. Experiments show that most of the laser energy on the substrate surface is distributed at the center and the outmost ring. Optical microscope and scanning electron microscope (SEM) observations reveal that concentric ring structures are only formed on the substrate surface at the positions between the focus plane and the lens. Both the outmost ring diameter and the ring number increase with the defocus distance, however, they are not dependent on laser fluence. This phenomenon could be attributed to the lens pupil truncation and its aberration. Laser energy concentrated at the outmost ring can be used to punch via microholes with the diameter determined by the defocus distance. This technique provides a high-speed, high-efficiency manufacturing method for via microhole array fabrication with low-energy laser ablation. [DOI: 10.1143/JJAP.42.5123]

KEYWORDS: laser ablation, truncated Gaussian beam, diffraction rings, spherical aberration, via microhole drilling

1. Introduction

Pulsed laser ablation of polymer substrates has attracted a great deal of interest in recent years.[1,2] Kapton polyimide film is one of the popular laser-processed polymers due to its excellent electrical and mechanical characteristics, and temperature stability.[3] Precision excimer laser drilling is currently the routine process in industries for fabricating microholes for connections in IC chips and inkjet printer nozzles.[4] However, disadvantages such as the usage of toxic and corrosive gases, poor beam quality, low repetition rates, high maintenance cost and expensive masks limit the extensive use of the excimer lasers. Nd:YAG lasers with high repetition rates and Gaussian TEM_{00}-mode beam can be used as an alternative for mask-free drilling.[5] In general, the laser beam maintains its energy spatial distribution in a Gaussian profile for the laser ablation.[6] Within the irradiated region, the laser energy higher than the ablation threshold energy causes the material removal. The profile of an ablated hole is truncated at the edge where the energy is equal to the threshold value for material removal. Due to the Gaussian energy distribution, the ablation depth at the edge is lower than that at the inside area. For high-speed laser processing, it is highly desirable to distribute most of the energy at the ablated edge. To date, many techniques have been conducted with the aim to modify the Gaussian beam profile.[7–12] Most reported works focus on attempts to flatten the laser beam profile. For this ablation scheme, the laser energy intensity distribution is uniform resulting in the same ablation rate throughout the whole irradiated area, it is suitable for fabricating structures with controlled ablation depth, such as the blind hole drilling. However, for the flat energy profile, most of the energy is contributed to ablate the materials inside the irradiated area instead of just the area edge, a technique to concentrate the laser energy at the hole edge is one of the best options for low-energy-laser direct via drilling. The hole is punched down with the inside area unaffected, which can increase the processing efficiency greatly due to the fact that a much smaller amount of material is ablated away. Efficient results can be obtained with interference beam shaping, but the required optical setup is very complicated.

In this paper, we report a phenomenon of producing laser-ablation-induced concentric ring structures, which are formed onto the substrate surface at defocus planes. Experimental results indicate that the laser energy can be confined in the area of the structure to have most of the laser energy concentrated at the center and the outmost ring. A laser-punching method is proposed to fabricate microholes by low-energy Nd:YAG lasers. The edges of the holes are defined by the laser ablation at the outmost ring. Via holes with different diameters are obtained on Kapton surface by simply adjusting the defocus distance.

2. Experimental

The light source used is a 3rd harmonic Nd:YAG laser (Coherent AVIA 355-1500, 30 ns) with TEM_{00} mode. The laser light, after passing through a beam expander, was measured by a laser beam analyzer (Spiricon LBA-300PC) to ensure that the output beam is a Gaussian beam. The laser beam is then focused by an uncoated Plano-Convex lens (focal length = 25 mm). Output aperture diameter of the lens is 2 cm. The repetition rate of laser pulses was kept at 1 kHz for all the experiments. The laser was operated in the burst mode with selected pulse number in the range from 1 to 65,000. The sample was mounted on a three-dimensional X–Y–Z translation stage with its surface perpendicular to the incident laser beam. The Z-stage changed the distance between the lens and sample surface. Laser ablation was carried out on commercial polyimide films with thickness of 50 μm (Dupont Kapton). Laser pulse energies were calibrated using an energy meter (OPHIR PE10-SH). The fluences can be changed by tuning the pulse energy or the irradiated area, the latter of which can be achieved by moving the sample along the optical axis by the Z-stage.

3. Results and Discussion

Figures 1(a)–1(f) show scanning electron microscope (SEM) micrographs of the ablated region on the Kapton surface at different pulse numbers, the sample surface was kept 700 μm above the focus plane. When the AVIA laser is operated at the burst mode, the energy of the first pulse is extremely low, which could be due to the fact that the energy is building up. By measuring the energy output, it is found that the pulse energy will become stable after the second

*E-mail address: HONG_Minghui@dsi.a-star.edu.sg

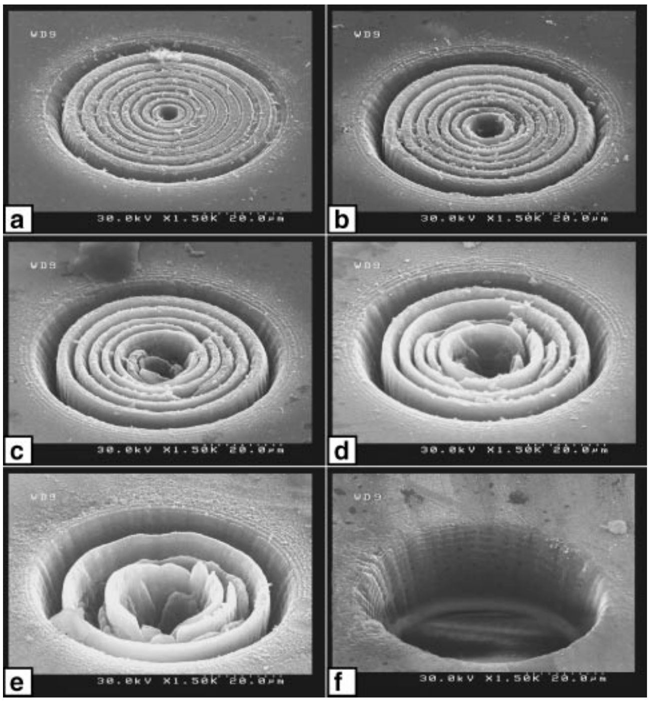

Fig. 1. SEM micrographs of concentric ring structure formed on Kapton surface at laser fluence of $2\,\mathrm{J/cm^2}$ obtained at different pulse numbers: (a) 2, (b) 5, (c) 10, (d) 20, (e) 50 and (f) 100. The sample is placed $700\,\mu\mathrm{m}$ above the focus plane.

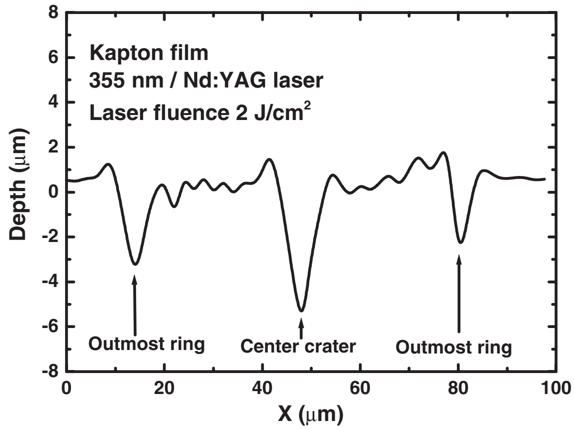

Fig. 2. Ablation surface profile of Kapton after 10 pulses of 355 nm Nd:YAG laser irradiation at a laser fluence of $2\,\mathrm{J/cm^2}$. The sample is placed $700\,\mu\mathrm{m}$ above the focus plane.

pulse. Therefore, at least two laser pulses were applied to irradiate the sample surface. The laser fluence applied was $2\,\mathrm{J/cm^2}$ with 2, 5, 10, 20, 50, and 100 pulses. In Fig. 1(a), it can be observed that the ablated structure has a deep central crater with a diameter of $6.4\,\mu\mathrm{m}$, outside of which 8 concentric rings with diameters of 9.6, 14.6, 20.7, 25.9, 32.4, 39.3, 47.4 and $58.7\,\mu\mathrm{m}$ are formed. The widths of these 8 ablated rings also increase along the radial direction from the center, and are 0.86, 1.0, 1.07, 1.14, 1.2, 1.29, 1.86 and $5.14\,\mu\mathrm{m}$. The widths of the two outmost rings are obviously larger than the others. Furthermore, it can be observed that the groove of the outmost ring (the 8th ablated ring) is much deeper than those of the other 7 ablated rings. The areas at the spacings between the ablated rings are not damaged by the laser irradiation except some laser ablation debris on their surface. It demonstrates that the laser intensities at the position between the ablated rings are not sufficiently high for material removal. Therefore, it can be concluded that the laser beam profile changes from that of the Gaussian beam to the special distribution by the optical lens. In Figs. 1(b)–1(e) the increasing widths of the central crater are 9.2, 12.4, 19.6 and $28.6\,\mu\mathrm{m}$ and the decreasing ablated ring numbers are 7, 6, 5 and 2, respectively. It is found that the diameter of the outmost edge does not increase with pulse number, but its depth increases greatly. To obtain the ablated profile information, the sample surface morphology was scanned by the surface profiler. Since the central craters of the first two figures are small and it is difficult to measure their depths accurately, the profile on Kapton surface ablated by 10 pulses of laser irradiation at a laser fluence of $2\,\mathrm{J/cm^2}$ [Fig. 1(c)] is shown in Fig. 2. It can be seen that the depths of the central crater and the outmost ring are $5\,\mu\mathrm{m}$ and $3\,\mu\mathrm{m}$, respectively, while the depths of other rings are much shallower than the outmost ring. Due to the strong absorption of UV light of Kapton materials, the formation of the ablated pattern is closely related to the laser energy distribution on the sample surface. It is clear that the 1st and 2nd highest laser energy intensities occur at the center and the outmost ring and the energy intensities at the other rings are much lower. By estimating the material volume removed by laser ablation and neglecting the energy at the spacings between the ablated rings, it is found that more than 70% of the laser energy is distributed to the outmost ring section. Furthermore, only 5 rings are observed after 10 pulses of laser irradiation. It is due to the fact that the widths of the central crater and the rings are enlarged to merge with the nearby rings as the number of pulses increases. After 100 pulses of laser irradiation, the substrate materials at the outmost ring are totally removed. A via microhole is obtained on the Kapton surface with the thickness of $50\,\mu\mathrm{m}$. Furthermore, it can be observed that at the fixed defocus position, the outmost ring diameter and the ring number do not change with laser fluence, while the ring width increases with laser fluence. For higher laser fluence, the increase of the ring width causes the ablated rings to merge together, not a concentric ring structure but rather, a circular ablated area with a well-defined edge is obtained.

The high energy concentration at the outmost ring could be due to the truncation effect of the lens aperture. Numerical calculation has shown that when the truncation effect is weak, the truncated Gaussian beam could still be considered a new Gaussian function when propagating.[13] Mahajan reported that the pupil radius must be at least three times the beam radius for a weakly truncated beam.[6] In this work, the pupil in front of the lens was not large enough to pass all of the illuminated light ($D_{\mathrm{aperture}} \approx D_{\mathrm{light}}$), the Gaussian function is truncated by the finite pupil to introduce edge diffraction effects, which cause the highest energy intensity at the central crater. The intensity at the outermost ring is always higher than those of other rings formed inside.

Figure 3 shows the ablated results on the Kapton surface obtained by changing the sample position along the optical axis. The positive z direction represents the optical axis toward the lens. The focus plane is located at $z = 0$. The

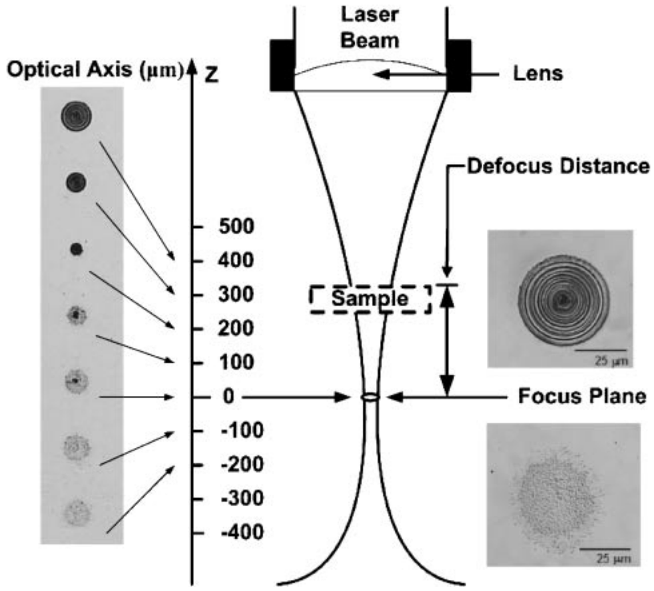

Fig. 3. Illustrations of the ablated patterns formed at different sample positions along the optical axis.

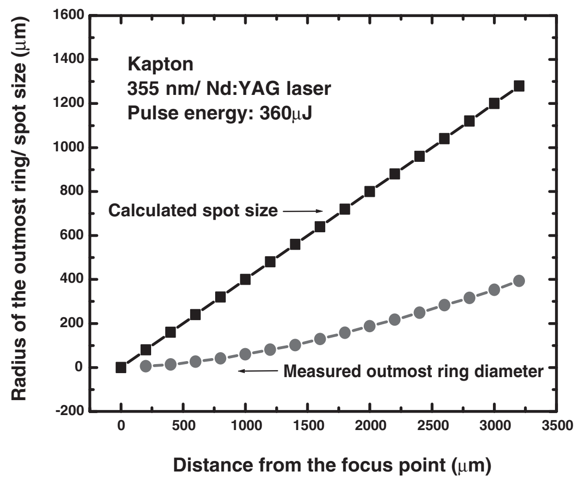

Fig. 4. Radius of outmost ring and laser spot size vs defocus distance from focus plane. The laser spot sizes are calculated from eq. (1).

defocus distance is defined as the value of z. Two laser pulses were applied to irradiate the sample surface. The sample position was changed at an increment of 100 μm. The ablated patterns are asymmetric for the samples located above and below the focus plane at the same defocus distance. When the sample is placed below the focus plane (z is negative), no obvious ring patterns are observed. When the sample is placed above the focus plane (z is positive), clear and sharp concentric ring structures are observed. Furthermore, the outmost ring diameter and the number of rings increase with the value of z. The minimum outmost ring diameter obtained is 3 μm. As the sample moves along the positive z direction, the images of the ring structure become weak. It is due to the increase of the laser-irradiated area, which reduces the laser fluence on the surface. At the position of +2400 μm, only the central crater and the ablated outmost ring with a clearly circular structure could be observed on the Kapton surface. The outmost ring diameter is about 500 μm corresponding to the laser fluence of 0.1 J/cm^2. The images are symmetric about the optical axis but asymmetric at each side of the focus point. The structure symmetry about the optical axis indicates that only on-axis factors can lead to the formation of the ring structures.

Figure 4 shows the radius of the pattern area, i.e., the radius of the outmost ring, compared with the beam spot size as a function of the distance from the focus point. The beam spot size can be estimated from the propagation law of a Gaussian beam as:[13)]

$$\omega_z^2 = (\lambda z/\pi\omega)^2 + \omega^2(1 - z/R)^2, \tag{1}$$

where ω_z is the beam radius at a distance z from the lens, λ is the laser wavelength, ω is the beam radius at the lens and R is the focus length of the lens.[6)] The diameter of the outmost ring is smaller than the calculated focused-beam spot size. By using an aperture in front of the focus lens to narrow the beam, it is found that when the diameter of the aperture decreased, the ablation at the center also decreased, while the rings at the outer region remained the same. When using an obstacle to shadow the center of the unfocused beam, only the center ablation could be found because the rings around the center would disappear. It could be due to the spherical aberration at defocus planes described in the optic imaging system.[14)] The spherical aberration, which originates from the spherical plane of the optical elements, is normally symmetric around the optical axis. In the presence of spherical aberrations, the focal lengths of the rays passing through the edge of the lens are always different from that determined by the paraxial rays, and the concentrations of edge rays located at one side of the focus point induce asymmetrical intensity distributions above and below the focal plane. In this case, clear images are located at the positions above the focus plane, and their sizes are smaller than the calculated beam spot size. It indicates that the edge rays form a shorter focus length, and the edge of the ablated structure is determined by the paraxial rays at defocus planes, which produces a smaller area than that by theoretically estimated.

Since the absorption coefficient of Kapton film at wavelength of 355 nm is 3.6×10^3 cm^{-1},[15)] it is expected that the incident laser energy will be deposited to a few micrometers below the surface and result in intense localized heating. The polymer will thermally decompose for laser energy higher than the threshold, resulting in efficient drilling. The steep intensity distribution at the outmost ring area confines the incident energy in a clearly distinct boundary and results in efficient removal of material. This phenomenon can be used to fabricate via microholes with the ablated edge defined by the high laser energy intensity at the outmost ring. It can be estimated that the total volume of removed materials necessary for a Gaussian beam to fabricate a via hole is about 10 times higher than this new laser ablation scheme. Compared with excimer laser drilling which consumes higher energy output to obtain the hole of the same size, the new ablation method has much higher drilling efficiency for via holes fabrication, and the optical setup is quite simple. The cost for microhole fabrication by AVIA laser is also much lower than the case of excimer laser because of the cost of equipment, the maintenance fee and the cost of mask preparation. Due to the high repetition rate of the Nd:YAG lasers, the time required for drilling one hole would be very short. For example, 0.1 s is enough time to drill a 50 μm hole on Kapton film at a repetition rate of 1 kHz and pulse energy of 60 μJ.

4. Conclusions

In summary, laser-ablation-induced concentric ring structures are investigated. The concentric ring structures are formed by laser ablation on substrate surface at positions between the focus plane and the lens. The ablation profile illustrates that the 1st and 2nd highest energy intensities occur at the center and the outmost ring, respectively. The outmost ring diameter and the ring number increase with the defocus distance, however, they are not dependent on laser fluence. Concentric ring structures could be resulted from the laser beam truncation and the spherical aberration of the optical elements. Laser ablation occurring at the outmost ring is used to punch via microholes with the diameter determined by the defocused distance, which demonstrates a low-cost, high-speed, highly efficient laser via drilling technique.

Acknowledgement

The authors would like to thank Professor B. Luk'yanchunk, Dr. D. J. Wu and Dr. C. W. An for their valuable discussions.

1) A. Ivarson, J. Powell and C. Magnusson: J. Laser Appl. **8** (1996) 191.
2) T. Lippert, C. David and M. Hauer: Appl. Surf. Sci. **186** (2002) 14.
3) R. Srinivasan: Appl. Phys. Lett. **58** (1991) 2895.
4) M. C. Gower: SPIE Proc. **3618** (1999) 251.
5) A. S. Holmes: SPIE Proc. **4274** (2001) 297.
6) V. N. Mahajan: *Optical Imaging and Aberrations* (SPIE PRESS, US, 1998) Part. 2, Chap. 4, p. 354.
7) P. E. Klingsporn: Appl. Opt. **15** (1976) 2355.
8) S. K. Dew and R. R. Parsons: Appl. Opt. **31** (1992) 3416.
9) R. M. Stevenson, M. J. Norman, T. H. Bett, D. A. Pepler, C. N. Danson and I. N. Ross: Opt. Lett. **19** (1994) 363.
10) X. Deng, X. Liang, Z. Chen, W. Yu and R. Ma: Appl. Opt. **25** (1986) 377.
11) J. X. Pu and H. H. Zhang: Appl. Opt. **37** (1998) 4200.
12) J. X. Pu, S. Nemoto and H. H. Zhang: J. Mod. Opt. **46** (1999) 1611.
13) K. S. Lee: Appl. Opt. **25** (1986) 3671.
14) M. Born and E. Wolf: *Principles of Optics* (Pergamon Press, UK, 1999) 7th ed., Chap. 9, p. 538.
15) D. Bauerle: *Laser Processing and Chemistry* (Springer, Berlin, 1996) 2nd ed., p. 580.